N90-22999

Algorithms for Computing the Multivariable Stability Margin

Jonathan A. Tekawy[*], *Michael G. Safonov*[†] *and Richard Y. Chiang*[‡]

Abstract

Stability margin for multiloop flight control systems has become a critical issue, especially in highly maneuverable aircraft designs where there are inherent strong cross-couplings between the various feedback control loops. To cope with this issue,we have developed computer algorithms based on non-differentiable optimization theory. These algorithms have been developed for computing the Multivariable Stability Margin (MSM). The MSM of a dynamical system is the "size" of the smallest structured perturbation in component dynamics that will destabilize the sytem. These algorithms have been coded and appear to be reliable. As illustrated by examples, they provide the basis for evaluating the robustness and performance of flight control systems.

1   Introduction

Accurate knowledge of the dynamical model associated with the design of modern flight control system is becoming more difficult to obtain. This is especially true for the design of the next generation fighters where many of the performance specifications go beyond the capability of the aircraft currently in service. Robust control analysis methods have received considerable attention in recent years as a possible solution to the problem of controlling systems for which the given model contains significant uncertainty [Saf 1] [Doyle2]. The central feature of these methods is their effectiveness in handling an unknown-but-bounded class of plants, instead of the nominal plant only.

[*]Flight Control Research, Aircraft Div., Northrop Corporation, Hawthorne, CA 90250
[†]E. E. - Systems Dept., University of Southern California, Los Angeles, CA 90089-0781
[‡]Flight Control Research, Aircraft Div., Northrop Corporation, Hawthorne, CA 90250

The uncertainty in the nominal plant arises from several different sources: For gain-scheduled aerospace vehicle control systems, typical uncertainties in the plant at each design point consist mainly of modeling errors due to uncertain aerodynamic coefficients, linearization, model reduction, neglected dynamics, time-delays, etc. Aerodynamic coefficients developed from wind tunnel testing or computational fluid dynamics usually are different from those obtained from actual flight data. Linearization will also affect the nominal plant behavior. Nonlinear effects such as actuator saturation and rate limits are neglected altogether when a model is linearized. Parameter drift will also affect the nominal plant. There may be dynamical modes which are intentionally or unknowingly neglected. In addition phase loss which results from time delay also leads to an uncertainty bound.

The uncertainty may be loosely classified as falling into two categories, structured and unstructured. Structured uncertainty arises from specific component or parameter variations. Two examples of structured uncertainty are variations in weight and drifting aerodynamic parameters. Unstructured uncertainty is any other sort of uncertainty which can be regarded as a frequency-dependent norm bounded perturbation matrix. High frequency modeling errors are one type of unstructured uncertainty. The linearization of the nonlinear equations of motion contribute to both classes of uncertainty. Actuator rate and position limits have a distinctive signature which can easily be isolated, so that they fall into the class of structured uncertainties. On the other hand, the effects of nonlinear kinematic terms can only be bounded, therefore necessitating an unstructured uncertainty representation.

2 Robustness Measure

Safonov [Saf 2], who built upon different, but related, conic-sector nonlinear stability theory work of Zames [Zames], reinterpreted the conic-sector stability concepts in order to deal with uncertainty and robustness issues. Safonov, Doyle and Fan, to name a few, have contributed to the continuing development in this area [Saf 3] [Saf 4] [Doyle2] [Fan].

Basically the robustness measure is done by lumping uncertain deviations from a nominal system $M(s)$ into an uncertain matrix $\Delta(s)$ resulting in an uncertain feedback system with loop transfer function $\Delta(s)M(s)$ as shown in figure 1.

Then, the Multivariable Stability Margin (MSM), "K_m", is defined as the smallest stable, norm-bounded perturbation $\Delta(s)$ that can destabilize the system. While K_m is in general difficult to compute, a reasonably tight lower bound $\underline{K}_m$ theoretically can be computed using diagonally scaled singular values [Saf 3] [Doyle2] [Fan]. The plot of $\underline{K}_m(w)$ vs. frequency identifies tolerable levels of parameter uncertainty as a function of frequency.
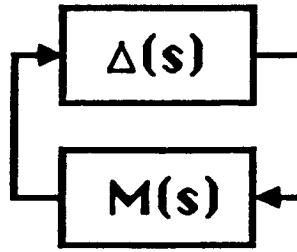
$$\Delta = \text{diag}[\Delta_1, \Delta_2, \ldots, \Delta_i, \ldots, \Delta_n]$$

Figure 1: Robustness analysis model.

For unstructured uncertainty, the maximum singular value has been shown to be useful in bounding the multivariable stability margin. However, the bound can be very conservative in the case of structured uncertainty. The singular value analysis will attempt to find the worst direction of the uncertainty that in reality impossible to exist. To deal with the case of diagonally structured Δ, Safonov [Saf 4] introduced the two-sided structured <u>Multivariable Stability Margin</u> (MSM), denoted K_m, and Doyle [Doyle2] introduced the term <u>Structured Singular Value</u> (SSV), denoted μ, to describe the reciprocal, $\mu(M(s)) = 1/K_m(M(s))$. Diagonal perturbations are quite general and flexible if one considers parametric uncertainties (e.g. aerodynamic coefficients). Traditionally one defines K_m and μ for "two-sided" magnitude-bounded uncertainties which may be either positive or negative; but in cases where the sign of the uncertain Δ_i is known a priori one may modify the definitions of K_m and μ accordingly.

When the uncertainties are known to cover both positive and negative perturbations, the SSV of Doyle and MSM of Safonov provide a "tight" (to within 15%) condition for robust stability. This condition is measured by representing directly the individual sources of uncertainties in the form of block diagonal perturbations.

Definition: Given transfer functions $G(s), a(s)$ and $b(s)$, we write

$$G(s) \in sector[a, b]$$

if

$$|G(jw) - C(jw)| \leq |r(jw)| \qquad \forall w$$

where

$$C(s) = (a(s) + b(s))/2$$

and

$$r(s) = (a(s) - b(s))/2$$

Assuming $M(s)$ and $\Delta(s)$ to be stable then the one-sided MSM, "K_{m_1}" and, the two-sided MSM, "K_{m_2}" are defined by the following (see figure 2 and 3):
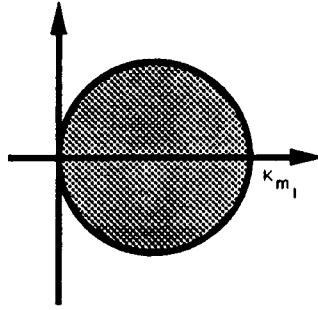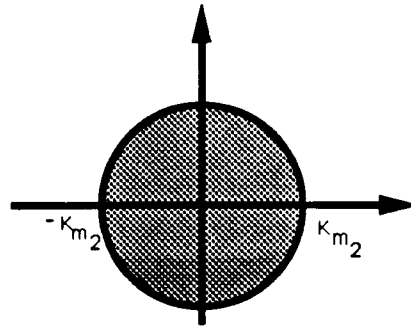
Figure 2: One-sided K_m

Figure 3: Two-sided K_m

- One-sided K_m :

  The system is stable for all Δ with

  $$\Delta_i \in sector[0, K_{m_1}] \quad \forall i = 1, \cdots, n. \tag{1}$$

- Two-sided K_m :

  The system is stable for all Δ with

  $$\Delta_i \in sector[-K_{m_2}, K_{m_2}] \quad \forall i = 1, \cdots, n. \tag{2}$$

For any diagonal matrix D, a practical upper bound on $\mu = 1/K_{m_2}$ is $\sigma_{max}(DMD^{-1})$. Further, it is known that for 3 or fewer Δ_i 's that the minimum over D of this upper bound is actually equal to μ [Doyle2]. Safonov and Doyle proved that the minimization problem of $\sigma_{max}^2(DMD^{-1})$ is convex in $D' = log(D)$, so that every local minimum is a global minimum. Furthermore, computational experience has shown that minimum of $\sigma_{max}(DMD^{-1})$ over D is within 15% of μ. So, we choose to work with this upper bound, $\underline{K}_{m_2}^{-1}$, to calculate the reciprocal of two-sided MSM. Practical upper bound for the reciprocal of one-sided MSM can be easily derived by using conic
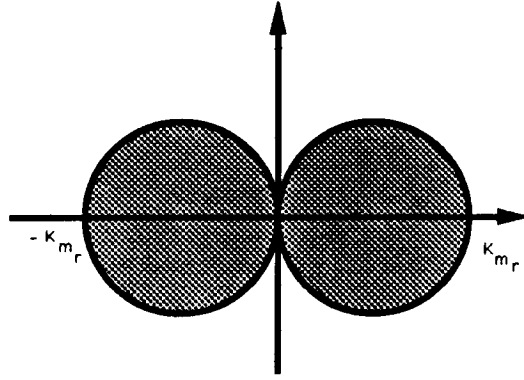
107

Figure 4: K_{m_r}

sector property of Zames [Zames]; viz. $K_{m_1}^{-1}$ is bounded above by

$$K_{m_1}^{-1} = max[\frac{1}{2}min_D\lambda_{max}(DMD^{-1} + (DMD^{-1})^*), 0] \qquad (3)$$

By modifying the former equation to include the permutation matrix ϕ_i, a less conservative bound for the two-sided real MSM, K_{m_r}, is given by

$$K_{m_r}^{-1} = max[\frac{1}{2}max_{\phi_i}min_D\lambda_{max}(DM\phi_iD^{-1} + (DM\phi_iD^{-1})^*), 0] \qquad (4)$$

Here

$$\phi_i \in \Phi, \quad i = 1, \cdots, 2^n$$

and Φ is the set of all permutation $n \times$ n diagonal matrices.

$$\Phi = diag[(\pm 1), \ldots\ldots, (\pm 1)]$$

The bound (4) is similar to the one proposed by Jones [Jones]:

$$\frac{1}{2}min_Dmax_{\phi_i}\lambda_{max}(DM\phi_iD^{-1} + (DM\phi_iD^{-1})^*) \qquad (5)$$

Although, equation (5) will lead to more conservative bounds. Geometrically equation (4) is shown in figure 4.

It should be mentioned at this point that several software packages are available to compute the two-sided MSM ,however , they are not accessible to the authors to be evaluated.

3 K_m Computation

The computation of σ_{max} is straight forward using available numerical software (Linpack). For both one-sided, real and two-sided cases, we have to solve an optimization

problem. However for all of these problems, the analytical gradient is available, so accurate solution can be obtained. However, when several eigenvalues or singular values coalesce (i.e., have multiplicity greater than one) the function is nondifferentiable ("creases" produce direction-dependent derivatives), so that a more complex algorithm of computing a descent direction is required. Before actually solving either case, one can approximately prescale the system matrix M by substituting for M the matrix DMD^{-1} where D minimizes the Frobenius norm of DMD^{-1} [Osborne].

The monotonic transformation of $D \rightarrow D'$, with $D = Exp(D')$, transforms the problem into a well behaved convex optimization [Saf 5]. The initial guess for D was taken to be equal to the identity. This initial guess was used only for the first frequency value in the given range. The solution obtained for a particular frequency point was then used as an initial guess for the next value. Suppose that the largest eigenvalue is simple, then a descent direction is calculated directly using the Davidon-Fletcher-Powell technique. In the case that the largest eigenvalue has multiplicity greater than 1 and the function is not continuously differentiable, a generalized gradient is used to determine a descent direction. Once this is done, the minimal point can be found in the specified descent direction by using a well known "binary search" algorithm of Bolzano. These steps are repeated until the global minimum is located (i.e. gradient is zero). Convexity of $\sigma_{max}^2(e^{D'}Me^{-D'})$ and $\lambda_{max}\frac{1}{2}(e^{D'}Me^{-D'} + (e^{D'}Me^{-D'})^*)$ ensures that this procedure is convergent to the global minimum. These steps can be summarized as follows:

1. Initialize $M_1 = M$; $D'_1 = 0$; $k = 1$.

2. Scale $M_{k+1} = e^{D'_k}M_k e^{-D'_k}$; set $D'_{k+1} = 0$

3. Find the search direction

   – Davidon Fletcher Powell (DFP) deflected gradient.
   – DFP generalized gradient for multiplicity ≥ 2

4. Unidirectional search.

   – Method of Bolzano (Fig. 5).

5. $D'_{k+1} \leftarrow D'_{k+1}+$ stepsize * search direction.

6. $k = k + 1$; go to step 2.

Step 5. of the algorithm involves varying the diagonal scaling matrix D' along a line by adjusting the scalar parameter stepsize. The size of $e^{D'_{k+1}}$ could approach the value of ∞. To prevent this, as the stepsize grows, M_{k+1}, is repeatedly updated to $M_{k+1} \leftarrow e^{D'_{k+1}}Me^{-D'_{k+1}}$ and stepsize and D'_{k+1} are reset to zero. This is done as often as needed to prevent numerical overflow when $e^{D'_{k+1}}$ is evaluated.
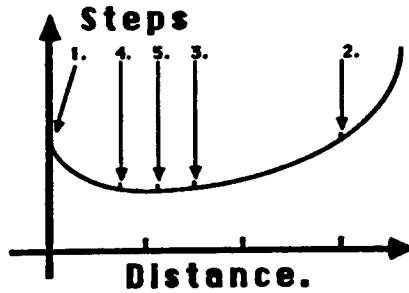
Figure 5: Method of Bolzano.

3.1 Generalized Gradient.

This discussion is not at all self contained and only key results will be stated. An excellent reference for this algorithm is [Polak]. In the case where the greatest eigenvalue/singular value has multiplicity greater than one, the function ceases to be differentiable. In this case the gradient is not defined and more complicated "generalized gradient" methods must be used to compute the descent direction. The generalized gradient at a nondifferentiable point is defined as the nearest point to the origin in the convex-hull of the set of directional derivatives at neighboring points; thus the computation of the generalized gradient at any point is itself a convex nonlinear programming problem. We employ an algorithm similar to that of [Doyle2, Polak1] to compute the generalized gradients of $\sigma^2_{max}(e^{D'}Me^{-D'})$ and $\lambda_{max}\frac{1}{2}(e^{D'}Me^{-D'} + (e^{D'}Me^{-D'})^*)$. Geometrically the algorithm is shown in figure 6 and summarized as follows:

- Generalized Gradient is defined as:

$$\nabla_{gen} \stackrel{\triangle}{=} N_r(Co\{\nabla(x)| \ \|x\| = 1\})$$

  where

  Co(.) - the convex hull of the set (.).

  Nr(.) - the nearest point to the origin of the set (.).

  $\{\nabla(x)| \ \|x\| = 1\}$ - the set of directional derivatives.

- Iterative algorithm for computing ∇_{gen}:

  1. Initialize $k = 1$.

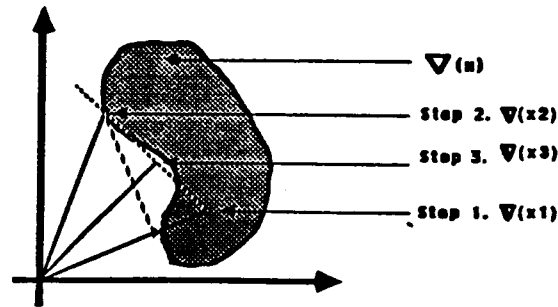 2. Guess x_k and set $y_k = \nabla(x_k)$.

Figure 6: Generalized gradient.

3. Find x_{k+1} by minimizing $(y_k^* \nabla(x_{k+1}))$ subject to $\|x_{k+1}\| = 1$.

4. Find $y_{k+1} = \text{Nr}(\text{Co}(y_k, \nabla(x_{k+1})))$.

5. Increment $k \leftarrow k + 1$, go to step 3.

3.2 Davidon-Fletcher-Powell Scaling.

The unmodified generalized gradient determines a steepest descent direction. The steepest descent direction is simply minus the generalized gradient. Steepest descent usually works quite well during early stages of the optimization process but if the Hessian (second derivative) matrix has a large condition number, the method usually behaves poorly, and small zig-zagging steps, called "stitching", take place (see fig. 7). Stitching problems also occur when the multiplicity of σ_{max} or λ_{max} is 3 or more. Therefore we use the Davidon-Fletcher-Powell (DFP) method to modify the generalized gradient in order to handle this phenomenon. This technique uses the previously calculated generalized gradient to estimate the Hessian and effectively rescale the function to make its Hessian better conditioned. This quadratic fit method requires fewer gradient evaluations and tends to converge faster. It should also be noted that the likelihood of stitching-induced premature termination of the algorithm (as can occur in the unscaled steepest descent technique) can be greatly reduced with the DFP scaling.

4 Lateral Directional Flight Control Example
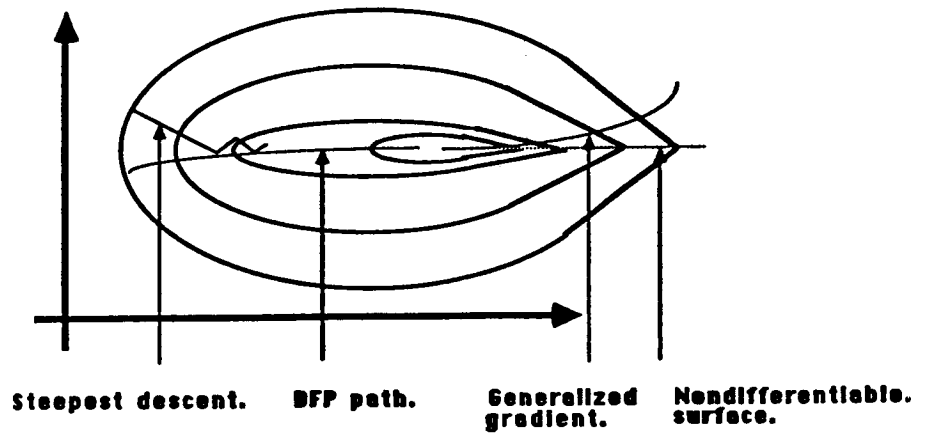
4.1 Example 1
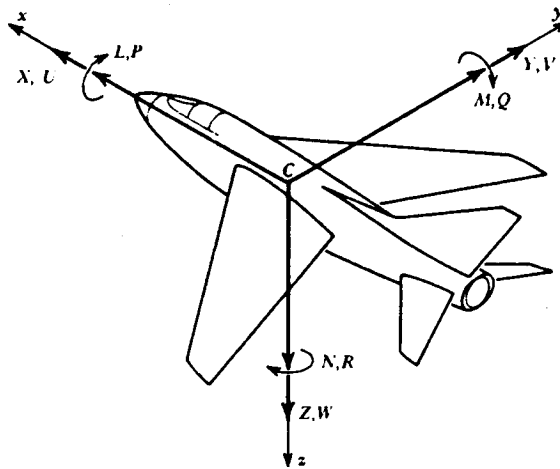
Figure 7: Minimization paths.
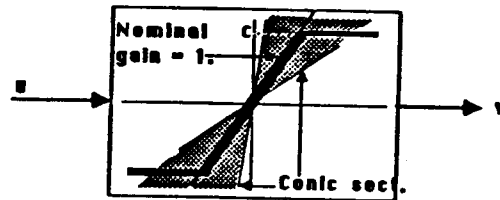

Figure 8: Axis systems and sign convention

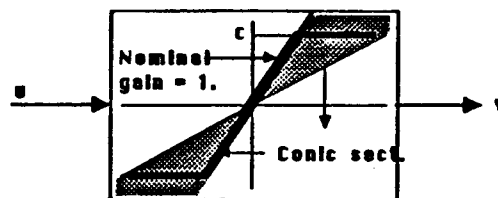Figure 9: Two-sided actuator uncertainty model.

Figure 10: One-sided actuator uncertainty model.

Nonlinear elements of actuators can be treated as linear conic-sector elements with structured uncertainty. This uncertainty can be modeled as one-sided or two-sided uncertain gains within the actuator model. This can be shown through an example. Consider a saturation curve below. If the input size is always less than C, then the saturation element is equivalent to a gain element with a magnitude of one, however, if u exceeds C, one may model the saturation element as a two-sided uncertain gain Δ in parallel with a nominal gain of one as shown in figure 9. A better approach is to model the saturation element by a gain with a nominal value of one and a one-sided negative uncertainty as shown in figure 10. Clearly, the one-sided model will produce less conservative margins than the two-sided model.

A design example is presented below in which MSM algorithm is asked to check the robustness of a typical lateral/directional flight control systems with respect to the actuator uncertainty (e.g. position saturation) and the reduction in the effectiveness of all control surfaces. The state-space matrices are given in figure 11. The controller uses roll rate, P, yaw rate, R, and the lateral acceleration, N_y, for feedback (see figure 12). By putting "extender wires" on the uncertainty blocks Δ_i and pulling them out into a separate "block", one can check the system robustness.

The plot of $\underline{K}_{m_1}$, $\underline{K}_{m_2}$ and σ_{max} are in figure 13. Note that the σ_{max} and $\underline{K}_{m_2}$ which have the minimum values of .015 and .42 respectively are equal or less than $\underline{K}_{m_1}$ for all frequency, and therefore shown to be more conservative than one-sided

A	B
C	D

$=$

-3.4d-1	-4.8d-1	-2.8d+2	3.2d+1	0.0d+0	-9.2d-4	-6.8d+0
5.2d-3	-3.0d+0	4.6d-1	-8.3d-6	0.0d+0	1.2d+1	-7.2d-2
1.5d-2	-1.4d-1	-1.9d+0	-7.5d-7	0.0d+0	3.8d-1	3.2d+0
0.0d+0	1.0d+0	0.0d+0	0.0d+0	0.0d+0	0.0d+0	0.0d+0
0.0d+0	0.0d+0	1.0d+0	0.0d+0	0.0d+0	0.0d+0	0.0d+0
0.0d+0	5.7d+1	0.0d+0	0.0d+0	0.0d+0	0.0d+0	0.0d+0
0.0d+0	0.0d+0	5.7d+1	0.0d+0	0.0d+0	0.0d+0	0.8d+0
-6.3d-3	-3.6d-2	7.5d-1	5.1d-8	0.0d+0	6.2d-2	1.6d-1

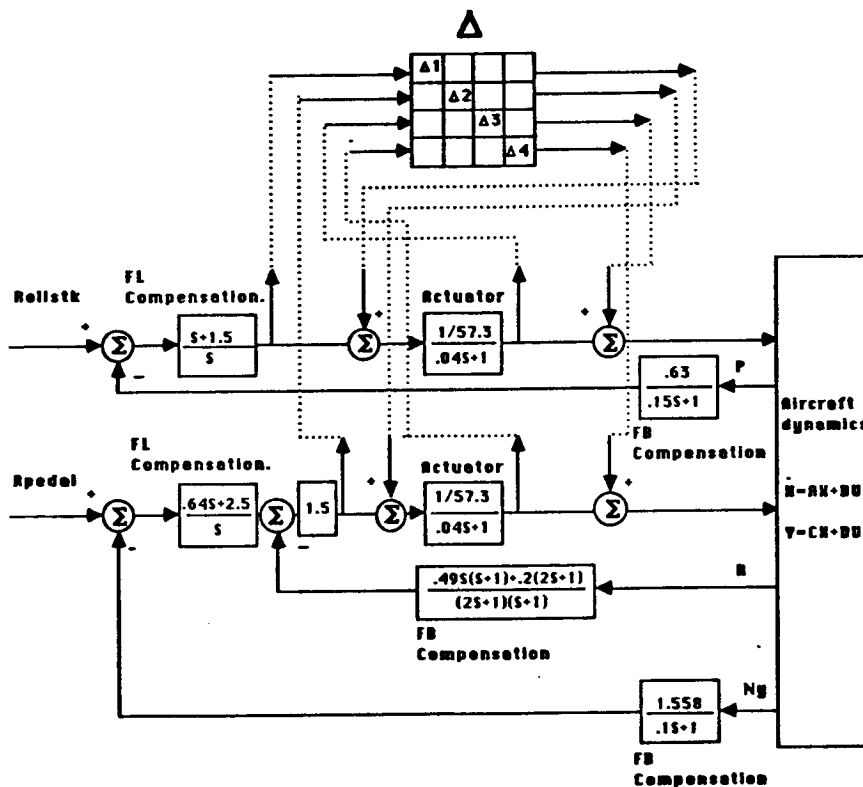Figure 11: State-space matrices.

Figure 12: Lateral directional flight control with uncertainties at the controller output and plant input.
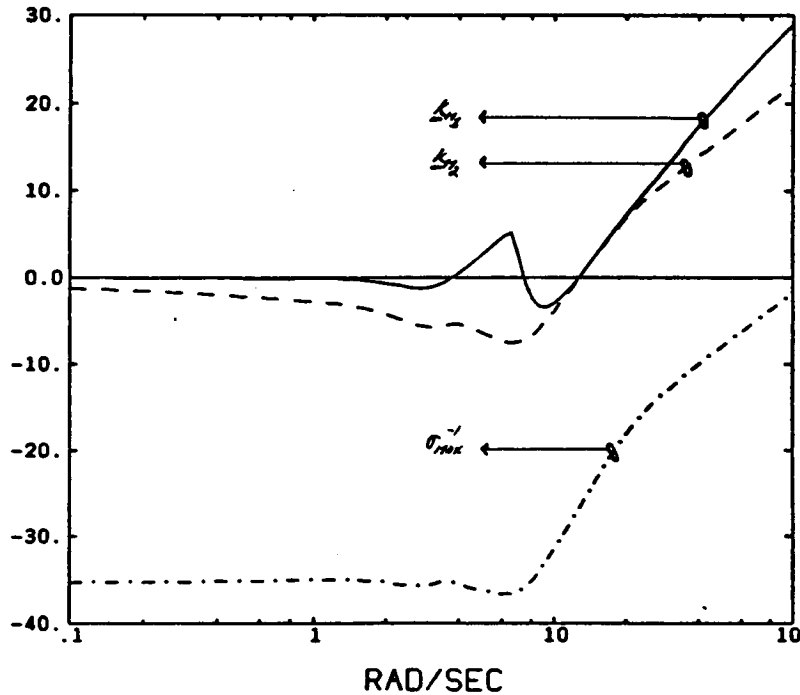
114

RAD/SEC

Figure 13: MSM at the plant input and controller output.

structured stability margin $\underline{K}_{m_1}$. This results from the one-sided structured multiplicative uncertainty that is not accounted for in the computation (i.e. nonlinear elements of actuators and gain reduction tolerance at the controller outputs). To properly account for the sign of the uncertainty and its structural information, the one-sided MSM was computed and it is shown to have a better robustness measure. $\underline{K}_{m_1}$ has the minimum value of 0.677, indicating that the system can simultaneously tolerate at least a 67.7 percent reduction in the effectiveness of all control surfaces and the actuator inputs up to at least three times the saturation value without instability.

4.2 Example 2

The MSM's minimal value $\underline{K}_{m_{peak}}$ also can be used to quantify a control systems tolerance of <u>simultaneous</u> gain and phase variations at <u>all</u> the plant inputs and outputs. This is done so the system has good stability robustness with respect to the uncertainties at the two actuator commands and the three sensor outputs (see figure 14). These uncertainties come from various sources. Model accuracy deteriorates at higher frequencies due to unmodeled aeroservoelastic effect. Several potential error sources exist within the assumed perfect sensors. Model reduction of the actuators can also be considered as one of the effects at the plant inputs.

Shown in figure 15 is the Bode plot of the MSM vs. frequency. The minimal value, denoted $\underline{K}_{m_{2_{peak}}} = .4196$, gives an indication of the minimal size of structured perturbations required to destabilize the system or equivalently diagonal perturbation
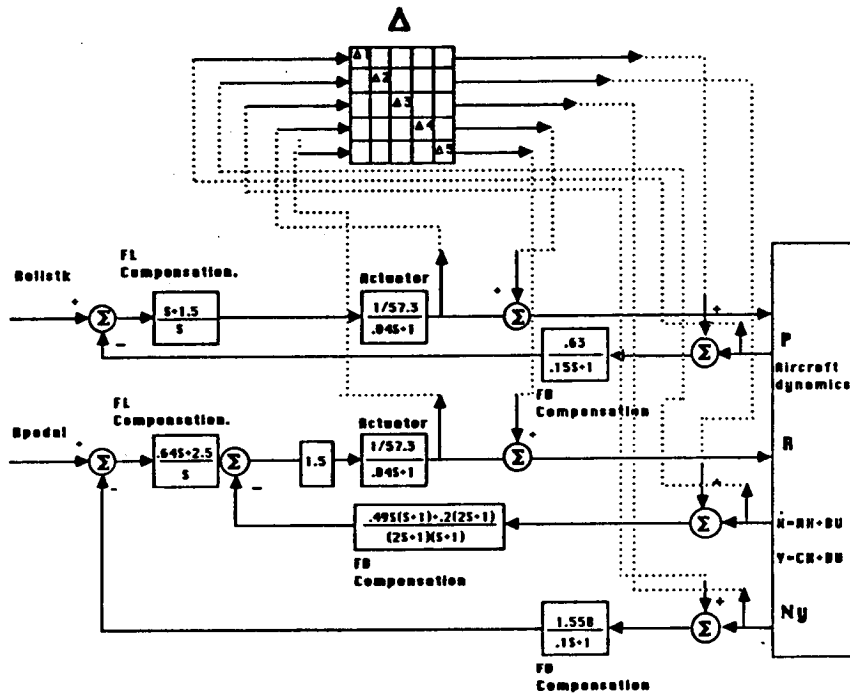
115

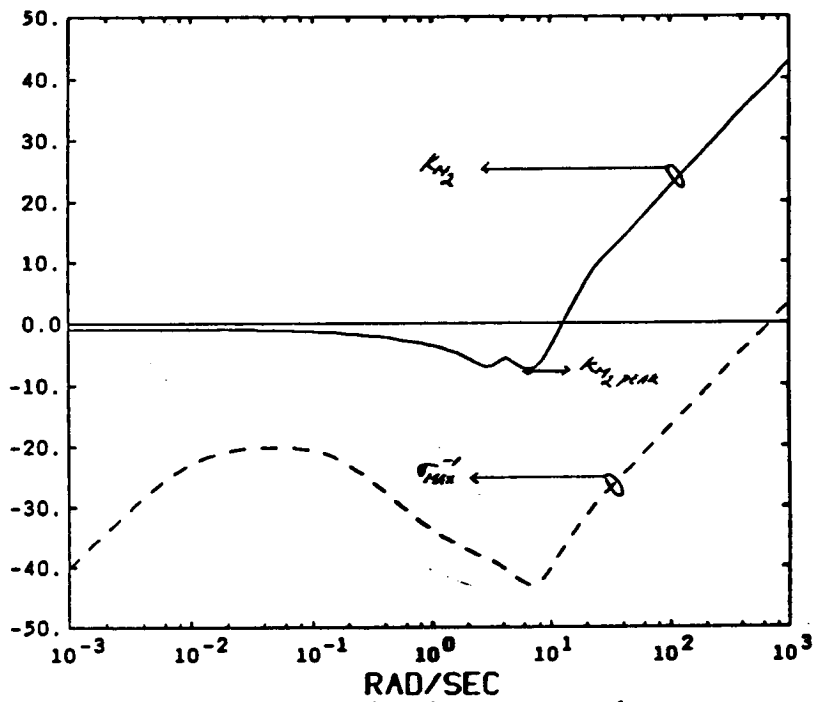Figure 14: Lateral directional flight control with uncertainties at the plant input and output.

Figure 15: MSM at the plant input and output.

as large as 41.96 percent can be tolerated at any frequency; at higher frequencies, perturbation magnitude as large as $w/10$ can be tolerated.

5 Conclusion

Computer algorithms for determining the multivariable stability margin "K_m" have been developed. The algorithms provide a reliable tool for evaluating the robustness of control systems with significant gain and/or parameter uncertainties. The computation for the one-sided and two-sided structured stability margin were done using nondifferentiable optimization theory. Robustness analysis was performed on a typical lateral directional flight control system problem with large uncertainty.

References

[Doyle2] Doyle, J. C. (1982a). Analysis of feedback systems with structured uncertainties. *IEE Proc.*, **129**,part D, 242-250.

[Fan] Fan, M. K. and Tits, A. L. (1986). Characterization and Efficient Computation of the Structured Singular Value. *IEEE Trans. on Automatic Control*, **AC-31**, 734-743.

[Jones] Jones, R. D. (1987). Structured Singular Value Analysis for Real Parameter Variations. *1987 AIAA Conference in Guidance and Control*.

[Osborne] Osborne, E. E. (1960). On pre-conditioning of matrices. *JACM*, vol. **7**, 338-345.

[Polak] Polak, E. and Mayne, D. Q. (1981). On the solution of singular value inequalities over a continuum of frequencies. *IEEE Trans. on Automatic Control*, **AC-26**, 690-694.

[Saf 1] Safonov, M. G., A. J. Laub and G. Hartmann (1981). Feedback properties of multivariable systems: The role and use of the return difference matrix. *IEEE Trans. on Automatic Control*, **AC-26**, 47-65.

[Saf 2] Safonov, M. G. (1980). *Stability and Robustness of Multivariable Feedback Systems*. MIT Press, Cambridge, MA.

[Saf 3] Safonov, M. G. (1982). Stability margins of diagonally perturbed multivariable feedback systems. *IEE Proc.*, **129**,part D, 251-256.

[Saf 4] Safonov, M. G. and M. Athans (1981). A multiloop generalization of the circle criterion for stability margin analysis. *IEEE Trans. on Automatic Control*, **AC-26**, 415-422.

[Saf 5] Safonov, M. G. and J. C. Doyle (1983). Optimal scaling for multivariable stability margin singular value computation. *Proc. MECO/EES'83 Symposium*, Athens, Greece.

[Zames] Zames, G. (1966). On the input-output stability of time-varying nonlinear feedback systems - Parts I and II. *IEEE Trans. on Automatic Control*, **AC-11**, 228-238 and 465-476, 1966.